

A method for automatic detection and classification of stroke from brain CT images

Mayank Chawla, Saurabh Sharma, Jayanthi Sivaswamy, Kishore L.T

mayank_c@research.iiit.ac.in

Abstract—Computed tomographic (CT) images are widely used in the diagnosis of stroke. In this paper, we present an automated method to detect and classify an abnormality into acute infarct, chronic infarct and hemorrhage at the slice level of non-contrast CT images. The proposed method consists of three main steps: image enhancement, detection of mid-line symmetry and classification of abnormal slices. A windowing operation is performed on the intensity distribution to enhance the region of interest. Domain knowledge about the anatomical structure of the skull and the brain is used to detect abnormalities in a rotation- and translation-invariant manner. A two-level classification scheme is used to detect abnormalities using features derived in the intensity and the wavelet domain. The proposed method has been evaluated on a dataset of 15 patients (347 image slices). The method gives 90% accuracy and 100% recall in detecting abnormality at patient level; and achieves an average precision of 91% and recall of 90% at the slice level.

I. INTRODUCTION

Stroke is a disease which affects vessels that supply blood to the brain. A stroke occurs when a blood vessel either bursts or there is a blockage of the blood vessel. Due to lack of oxygen, nerve cells in the affected brain area is not able to perform basic functions and cause sudden death. Stroke results in serious long term disability or death. According to the World Health Organization, 15 million people suffer from stroke, of these 5 million die and another 5 million are permanently disabled [1]. Strokes are mainly classified in two categories: 1) Ischemic stroke or infarct (due to lack of blood supply) and 2) Hemorrhagic stroke (due to rupture of blood vessel). Between these, ischemic stroke accounts for about 80 percent of all strokes [1]. However, it is also possible that both these types co-occur. During treatment, differentiation between ischemic and hemorrhagic stroke is of fundamental importance.

Computed tomography (CT) and magnetic resonance imaging (MRI) are the two modalities that are regularly used for brain imaging. CT imaging is preferred over MRI due to wider availability, lower cost and sensitiveness to early stroke. In most instances, CT provides information required to make decisions during emergency [2]. In CT images, a hemorrhage appears as a bright region (hyper dense) well contrasted against its surrounds. On the other hand, an ischemic stroke appears as a dark region (hypo dense), with the contrast

relative to its surround depending on the time elapsed since the stroke occurred. Sample images are shown in Fig. 1. The contrast starts by being poor in the early stages and improves over time as seen in Fig. 2. This is due to the fact that the density of the infarct region changes with the passage of time until it approaches the density of the cerebro-spinal fluid (CSF). Fig. 2 shows instances of early and late-stage of ischemic stroke.

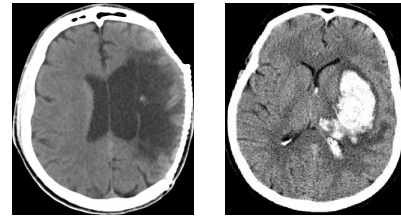


Fig. 1. (a) Ischemic stroke (shown as dark black area), (b) Hemorrhagic stroke (shown as bright white area).

Automatic detection of stroke is thus challenging as the structures vary in contrast with time and shape (see Fig. 3(a)). Complex combinations as shown in Fig. 3(b) can also occur.

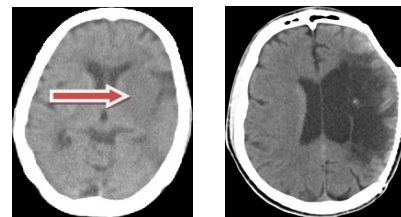


Fig. 2. CT exhibiting (a) early stage infarct (as pointed by arrow), (b) an old infarct (dark region)

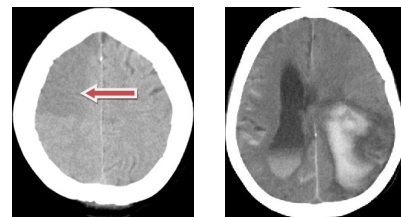


Fig. 3. (a) acute infarct (as pointed by arrow) (b) Hemorrhage (bright region) with infarct like edema (dark region)

M.Chawla, S.Sharma and J.Sivaswamy are with the Centre for Visual Information Technology, International Institute of Information Technology, Hyderabad, India

Kishore L.T is with the Institute of Medical Sciences, CARE Hospital, Hyderabad, India

slice. Accordingly, we characterize stroke as a distortion between the two halves of the brain in terms of tissue density and texture distribution. The novel feature with our approach is that it is able to distinguish between acute, chronic infarcts and hemorrhages, which has not been addressed by any previous work. In the next section, we briefly review the existing work on stroke detection from non-contrast CT data.

II. RELATED WORK

Most existing work on stroke detection mainly focus on hemorrhagic stroke detection. The approach in [3] exploits the fact that the hemorrhagic tissues are brighter than the normal tissues and hence uses a histogram-based k-means initial clustering followed by final segmentation using 3D morphological binary dilation of the initial clusters. Knowledge based approaches have been proposed in [4] and [5]. An unsupervised fuzzy clustering and expert system-based labeling of pixels is performed in the former while thresholding and morphological operations are done to segment candidate regions in the latter. The hemorrhagic candidates are then subjected to a knowledge based classification system that makes use of various image and anatomical features to separate the artifacts from the detected hemorrhagic candidates. A more comprehensive review of other methods for hemorrhage analysis can be found in [6]. More recently, wavelet-based texture analysis has been used to first eradicate all the nasal cavity slices followed by intensity based thresholding [7] to identify the stroke-affected regions.

In comparison to hemorrhagic stroke, considerably less attention has been paid towards detection of ischemic stroke due to its challenging nature. Suspicious regions are identified heuristically in [8] assuming the abnormal region would have grey values which are outliers compared to normal brain pixels. Further, assuming the abnormality can occur only on one side of the brain, symmetry is used to identify a set of suspicious pixels and later classified as abnormal based on connectivity. However, clinical data indicates that stroke can occur bilaterally in the brain, which invalidates the above assumption. Methods for segmenting and enhancing infarcts from given CT slices have also been reported in literature. Texture features are used to identify and segment infarcts in [9] while a rule based approach has been used in the latter in [10]. Solutions for curvelet-based enhancement of the early stage infarct has been proposed in [11]. Thus, based on the above it appears that the problem of detecting both type of strokes in a given CT volume has not been addressed.

III. PROPOSED METHOD

We model our approach based on the procedure followed by the radiologists who detect abnormality by examining the dissimilarity between the left and right hemispheres of the brain. Hence, in our approach, we relate the appearance changes in the two hemispheres to the changes in the overall shapes of their respective histograms. The shapes of the histogram is markedly different for chronic and hemorrhagic stroke cases since they affect the lower and higher end of the greyscale respectively. Histogram-based comparison is

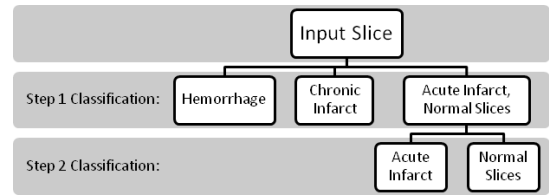


Fig. 4. Classification flowchart.

therefore used to identify these two cases. In contrast, the acute and normal cases are not so easily distinguishable from their histograms. Wavelet energy-based texture information is used for this discrimination. To summarise, our strategy is to perform a 2-level classification as shown in Fig. 4. In the first level, a given slice is classified as belonging to one of 3 classes: C1 chronic infarct, C2 Hemorrhage and C3 Normal or acute infarct. In the second level, C3 is split into two subclasses: C31 acute infarct and C32 normal. We will now describe the details of the proposed algorithm.

The proposed algorithm has three main steps. In the first step, the given slice is enhanced and denoised. Next, the line of brain symmetry is determined and finally, the abnormal slices are detected. Since infarct can occur in the nasal cavity region (brain stem or cerebellum) these slices are also considered for stroke detection.

A. Image enhancement and noise filtering

Since the dynamic range of the Hounsfield unit (HU) values for CT images is very large (-1000 to +1000 HU), the first task is to select the appropriate range of gray level for extracting soft tissue regions. The relationship between gray level ($I(x, y)$) and HU given as:

$$HU = I(x, y) + intercept \quad (1)$$

where, the intercept value can be obtained from the meta information available in the DICOM header of CT volume data.

The histogram of a given slice consists of two major peaks corresponding to the background and soft tissue pixels. Since the HU values of the soft tissue are higher than that of the background (air), the higher intensity peak will correspond to the soft tissue region [12]. A windowing operation to stretch the contrast is performed with the above peak value (P) as the center and W (set to be 120 HU) as the width of the window:

$$I_{new}(x, y) = 255 * \frac{I_{original}(x, y) - (P - \frac{W}{2})}{W} \quad (2)$$

After windowing, noise removal is performed using Wiener filtering to remove the graininess from the image. A sample image and the result of the enhancement and the denoising is shown in Fig. 6.

B. Rotation Correction and Detection of line of symmetry

Since our approach is to compare histograms of the two hemispheres, it is necessary to correctly identify the line of symmetry. The physical structure of the skull is used to detect the rotation angle as well as the line of symmetry. The line

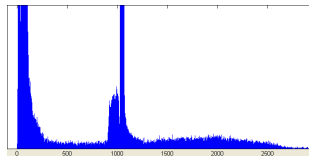


Fig. 5. Histogram of the CT image in Fig. 6 (a).

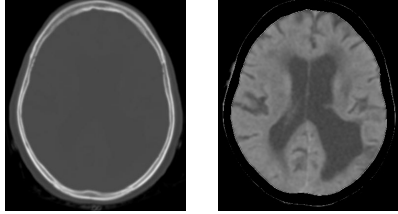


Fig. 6. (a) Original image, (b)Enhanced (windowed) image

of symmetry l_s is one that passes through the tip of the nose and bisects the horizontal line l_h passing roughly through the middle of the slice. We correct for any rotation present before extracting these lines. To find l_s we first search a set of slices (with high number of connected components) around the nasal cavity region. A sub-region is identified in these set of slices by locating the tip of the nose via a simple raster scan. The sub region is of size 30x512 and its horizontal projection profile is computed for every slice. The troughs in the profiles are found in either direction starting from the nose tip for each of the candidate slice. The slice which shows the most steep curve is chosen to be appropriate to detect and correct for rotation.

In the axial view, the nose appears as a hill with the tip being the peak of the hill and the base being bounded by knee points of the hill. In the absence of rotation, the line passing through the tip of the nose should be orthogonal to the line connecting the base of the nose. The knee points are easily detected by determining the rate of change of the slope of the nose boundary starting from the nose tip. The deviation of the base line from the horizontal gives the rotation angle which is used to perform a correction. This preceding step can only correct for rotation in the x-y plane. It is possible that the CT volume is also rotated in the axial direction which will mean the plane of symmetry will not be perpendicular to the x-y plane. Consequently, the lines of the symmetry for each slice will not align. In order to address this problem, we determine l_s for each rotation-corrected slice as follows: l_h is of same width as the horizontal projection profile of each slice and thus the required l_s is the bisector of l_h . A sample slice image and the result of rotation correction is shown in Fig. 7.

C. Detection of abnormal slices

The detection algorithm performs a 2-level classification to identify abnormal and normal slices. Histogram features are used in the first level while wavelet-based features are used for the second level. Since the nasal slices have very little soft tissue, they have to be handled with care. In our approach, they are classified as normal in the first level and passed to the second level for analysis.

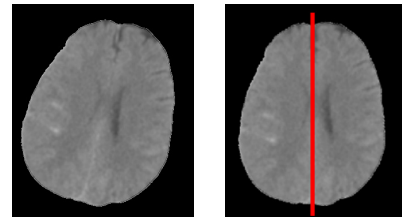


Fig. 7. (a) original image with rotation (b) rotation corrected image with the line of symmetry in red

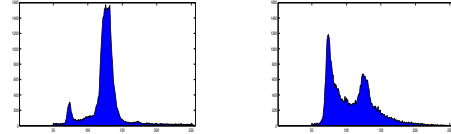


Fig. 8. Histograms of a hemisphere for (a) normal and (b) with an old infarct cases.

The first step differentiates the encephalic slices into three classes C1, C2 and C3 as described earlier, based on their histogram features. The l_s information is used to divide a slice into two hemispheres and the histogram for the right and left hemispheres are computed and compared for similarity. The similarity metric used is the correlation coefficient which is computed on a subsampled (by 5) version of the 2 histograms. Since only the low and high indexed bins are of interest, the measure is computed only for those bins. If this measure is below a threshold the corresponding bin number is noted. If the bin number is low, the slice is classified as belonging to C1 (see Fig. 8) and if the bin number is high the slice is classified as a member of C2. If the measure is below the threshold in both low and high indexed bins, the implication is that both type of abnormalities present in the slice. Therefore such slices are accorded membership in both C1 and C2. All slices with correlation measure above threshold are classified as belonging to C3.

In the second level of classification, the goal is to differentiate between normal and acute infarct cases. Histogram features are insufficient for this purpose as their grey value distributions overlap. This can be seen from the histograms shown in Fig. 9. Since the difference between the distributions are subtle, a finer analysis is required. A wavelet decomposition of the histograms is employed for this analysis. Daubechies-4 wavelet decomposition up to 5 levels are used to compute the energy distribution in the scale space. The corresponding energy values of the two histograms are compared using a simple difference of energy measure. If the difference is above a threshold, the slice is classified as belonging to C31. All other cases are classified as normal.

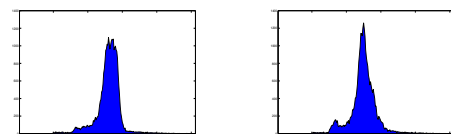


Fig. 9. Histograms of a hemisphere for (a) normal and (b) acute infarct cases.

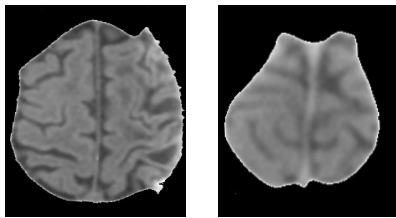


Fig. 10. Erroneous results: (a) False positive of normal (b) false positive of infarct categories

IV. EXPERIMENTAL RESULTS

The performance of the method has been tested on a dataset collected from a local hospital from two different scanners: Siemens Emotion 6 and Definition CT scanners. The dataset consists of volume CT data of 15 patients (6 normal and 9 abnormal - 6 infarct; 3 hemorrhagic) cases. Number and thickness of slices vary across patients: 18 – 31 slices and 4.8 – 6 mm, respectively. In total, there are 347 slices belonging to four main categories: 223 normal, 40 chronic infarct, 49 acute infarct and 35 hemorrhagic. Annotation for each slice of a CT volume was provided by a senior radiologist.

The classification performance of the proposed method was tested at slice and at patient (normal vs. abnormal case) level. The performance figures are presented in terms of precision (or positive prediction value) and recall (or sensitivity). At the patient-level if any slice is found to have an abnormality the entire volume is declared to be abnormal. Table II shows that the algorithm has 100% recall and 90% precision at the patient-level.

Table I presents the performance figures at the slice-level. The average precision obtained for individual category is 92% and maximum (93.3%) for hemorrhagic category. The average recall value is 90% and maximum (95.91%) for acute stroke category. In normal category, false positives were mainly due to mis-classification of slices at the boundary (in the axial direction) of the stroke. It can be seen from Fig. 10(a) that such slices do not show characteristics of abnormality and hence are difficult to classify. False negatives in the normal category arise due to a subtle difference between normal and acute stroke categories as seen in Fig. 10(b). Some regions of nasal cavity slices also appear close to infarct type mainly due to randomness of their histograms. The mis-classification rate can possibly be reduced with a better characterization of individual category.

	Normal	Abnormal / Stroke Slices		
Patients	6	9		
Slices (groundtruth)	223	Infarct		Hemorrhage
		Chronic	Acute	
True positive	205	38	47	28
False negative	18	2	2	7
False positive	17	4	4	2
Recall (%)	91.92	95.00	95.91	80
Precision (%)	92.34	90.47	92.15	93.33

TABLE I

PERFORMANCE FIGURES AT SLICE-LEVEL.

		Ground truth	
		Abnormal	Normal
Algorithm	Abnormal	9	0
	Normal	1	5
Recall		100%	
Precision		90%	

TABLE II

PERFORMANCE FIGURES AT PATIENT-LEVEL.

V. CONCLUSIONS AND FUTURE WORKS

In this paper, we have proposed an algorithm based on contra-lateral symmetry to detect stroke affected slices in a given CT volume. The key features of our algorithm are: ability to detect all types stroke (acute, chronic infarcts and hemorrhages) even if different types are present in the same slice. The proposed approach is a unified one which helps in building a stroke analysis system that can detect and segment all types of stroke. The contra-lateral symmetry condition that we have used fails when the same type of stroke occurs symmetrically in both hemispheres. Such cases, though rare, are currently not handled by our algorithm. Initial results obtained on testing over 347 slices are very encouraging. Most of the false positives in normal category can be reduced by using the fact that strokes are usually spatially continuous. Hence, if the imaging is done with thinner slices, continuity across slices can be an indicator for abnormality. As an alternative, it is possible to include some form of spatial information in the histograms, which can help detect symmetrically occurring strokes. Such information can also help in the stroke segmentation task.

REFERENCES

- [1] [Online]. Available: www.strokecenter.org/patients/stats.htm
- [2] [Online]. Available: stroke.ahajournals.org/cgi/content/full/38/5/1655
- [3] Atam, P. Dhawan, S. Loncaric, K. Hitt, J. Broderick, and T. Brott, "Image analysis and 3-d visualization of intracerebral brain hemorrhage," in *IEEE Symposium on Computer-Based Medical Systems*, 1993, p. 140145.
- [4] D. Cosic and S. Loncaric, "Computer system for quantitative analysis of ich from ct head images," in *19th Annual International Conference of the IEEE*, 1997.
- [5] T. Chan, "Computer aided detection of small acute intracranial hemorrhage on computer tomography of brain," in *Comput Med Imaging Graph*, Jun-Jul 2007.
- [6] N. Perez, J. Valdes, M. Guevara, and A. Silva, "Spontaneous intracerebral hemorrhage image analysis methods: A survey," *Advances in Computational Vision and Medical Image Processing*, 2009.
- [7] R. Liu, C. L. Tan, T. Y. Leong, C. K. Lee, B. C. Pang, C. Lim, Q. Tian, S. Tang, and Z. Zhang, "Hemorrhage slices detection in brain ct images," in *International Conference on Pattern Recognition*, Dec 2008, pp. 1 – 4.
- [8] E. Hudyma and G. Terlikowski, "Computer-aided detection of early strokes and its evaluation on the base of ct images," in *International Conference on Computer Science and Information Technology*, 2008, pp. 251–254.
- [9] A. Usinskas, R. A. Dobrovolskis, and B. F. Tomandl, "Ischemic stroke segmentation on ct images using joint features," *Informatica*, vol. 15, no. 2, 2004.
- [10] T. H. Lee, M. F. A. Fauzi, R. Komiya, and S.-C. Haw, "A rule-based approach to stroke lesion analysis from ct brain images," in *Image and Signal Processing and Analysis*, 2001.
- [11] K. Sklinda, P. Bargiel, A. Przelaskowski, T. Bulski, J. Walecki, and P. Grieb, "Multiscale extraction of hypodensity in hyperacute stroke," *Med Sci Monit*, 2007.
- [12] M. Matesin, S. Loncaric, and D. Petracic, "Unsupervised abnormalities extraction and brain segmentation," in *International Conference of Intelligent System and Knowledge Engineering*, 2008.